



Optimized and Sustainable Recovery of Ilmenite and Titanite from Low-Grade Rahba Placer Deposits: Integrating Physical Beneficiation Techniques

Mona M. Fawzy^{1*}, Mahinaz M. Shawky², Ahmed M. Ismail³, Mostafa Bayoumi⁴, Hassan Shahin⁵, Bahaa Emad⁶, Ahmed H. Orabi⁷, Gehan A.M. Aly⁸, Ahmed M. Abdelmouty⁹, and Mohamed Diab¹⁰

1. Physical Upgrading Department, Production Sector, Nuclear Materials Authority. P.O. Box 530, Maadi, Cairo, Egypt

2. Contracting Department, Contracts and Agreements Sector, Nuclear Materials Authority. P.O. Box 530, Maadi, Cairo, Egypt

3. Mineralogy Department, Research Sector, Nuclear Materials Authority. P.O. Box 530, Maadi, Cairo, Egypt

4. Remote Sensing Department, Contracts and Agreements Sector, Nuclear Materials Authority. P.O. Box 530, Maadi, Cairo, Egypt

5. Studies Department, Contracts and Agreements Sector, Nuclear Materials Authority. P.O. Box 530, Maadi, Cairo, Egypt

6. Radioactive Granitic Rocks Department, Research Sector, Nuclear Materials Authority. P.O. Box 530, Maadi, Cairo, Egypt

7. Analysis Department, Production Sector, Nuclear Materials Authority. P.O. Box 530, Maadi, Cairo, Egypt

8. Research Sector, Nuclear Materials Authority. P.O. Box 530, Maadi, Cairo, Egypt

9. Faculty of Computers and Information, Zagazig University, Zagazig, Egypt

10. Physical Upgrading Department, Production Sector, Nuclear Materials Authority. P.O. Box 530, Maadi, Cairo, Egypt

Article Info

Received 12 May 2025

Received in Revised form 5 June 2025

Accepted 6 August 2025

Published online 6 August 2025

DOI: [10.22044/jme.2025.16225.3141](https://doi.org/10.22044/jme.2025.16225.3141)

Keywords

Ilmenite

Titanite

Gravity concentration

Magnetic separation

Rahba

Abstract


In response to rising global demand for critical minerals and the need for environmentally responsible resource utilization, this study explores sustainable recovery methods from low-grade placer deposits in the Wadi Rahba area along the Southern Coast of the Red Sea of Egypt. The focus is on the beneficiation of ilmenite and titanite as primary valuable minerals. Twenty-eight samples, including a composite technology sample, were analysed using XRD, SEM-EDX, and ED-XRF techniques. Results indicate that total heavy mineral (THM) content ranges from 4.5% to 17.7%, averaging approximately 10%, with 11% in the composite sample. Identified valuable minerals include titanite, ilmenite, leucoxene, zircon, magnetite, and rutile, alongside high concentrations of heavy silicate minerals such as epidote, pyroxene, and amphiboles. Estimated contents are 0.44 wt.% titanite, 0.15 wt.% ilmenite, and trace amounts of zircon (0.04 wt.%), spessartine (0.01 wt.%), and magnetite (0.29 wt.%). To enhance recovery, a combination of gravity separation (Wilfley shaking table) and magnetic separation techniques (LIMS and HIMS) were applied. These methods effectively concentrated titanite and ilmenite, achieving recovery rates of 85.08% and 79%, respectively. The findings highlight the potential for economically viable extraction from low-grade sources using environmentally sustainable physical upgrading techniques.

1. Introduction

Low-grade placer deposits are becoming increasingly important due to rising demand for valuable minerals like gold, ilmenite, zircon, titanite, and rutile. These minerals are essential in high-tech industries, including electronics, aerospace, and renewable energy. As high-grade deposits are depleted, attention is shifting to lower-grade ones, which are often more accessible and economically viable due to advancements in extraction technologies [1–3]. Physical

beneficiation techniques like gravity and magnetic separation have improved mineral recovery, helping meet global supply needs while easing pressure on traditional mining operations [4–5].

Titanite and ilmenite are common in placer deposits due to their resistance to weathering. Titanite (CaTiSiO_5) contains titanium and rare earth elements, making it valuable for producing titanium dioxide pigments used in paints, plastics, and paper [6]. Ilmenite (FeTiO_3) is a primary

 Corresponding author: mm1_fawzy@yahoo.com (M. M. Fawzy).

source of titanium, crucial for manufacturing titanium metal and titanium dioxide, which widely used in aerospace and automotive industries [6].

In Egypt, placer deposits are found along the Nile River, the Mediterranean coast, and the Red Sea coast [7–14]. These deposits originate from the weathering and transport of mineral-rich parent rocks, containing ilmenite, zircon, rutile, titanite, magnetite, garnet, and leucoxene. Extracting titanite and ilmenite from Egyptian placer deposits has significant economic potential. Egypt's strategic location and rich geology make it an ideal mining site. The growing global demand for titanium—projected to rise from \$330.8 billion in 2023 to \$416.9 billion by 2030 (CAGR 3.4%)—further highlights the importance of these resources [15]. Developing these deposits can support sustainable resource use while protecting the environment.

To separate titanite and ilmenite, physical beneficiation techniques such as gravity, magnetic, electrostatic, and flotation separation are commonly used. Gravity separation (using shaking tables or spirals) exploits density differences between heavy minerals and lighter gangue [16–19] and [13,14]. Magnetic separation distinguishes ilmenite from non-magnetic minerals like titanite [20–23] and [11,12]. Electrostatic separation utilizes conductivity differences to enhance mineral separation [23]. Flotation is also widely employed in mineral beneficiation, leveraging differences in surface chemistry to selectively separate titanite and ilmenite under controlled pH and reagent regimes. This technique is particularly effective for the processing of minerals that are liberated at fine particle sizes, where conventional gravity or magnetic methods may be less efficient [24–28]. These physical techniques allow high recovery rates and high-purity products for industrial use while being environmentally friendly. Since they do not require harmful chemicals, they minimize pollution and ecosystem contamination. Additionally, they have less impact on water and soil compared to chemical or hydrometallurgical processes [29–31].

This study presents an approach to valorising low-grade stream sediment deposits from the Wadi Rahba area by integrating optimized physical beneficiation techniques—gravity and magnetic separation—to selectively recover valuable minerals, specifically ilmenite and titanite. Unlike conventional studies that focus on high-grade sources or rely on chemically intensive methods, this research demonstrates that environmentally sustainable, cost-effective physical methods can

yield high recovery rates (85.08% for titanite and 79% for ilmenite) even from marginal placer resources. The innovation lies in the strategic processing of fine-grained, mineralogically complex material through tailored separation parameters, establishing a scalable model for the sustainable exploitation of underutilized sedimentary deposits.

2. Sampling and Methodology

2.1. Sample locations

In this work, systematic sampling was conducted at 28 points along the middle of Wadi Rahba, a region extending in a northwest-southeast direction parallel to the Red Sea coast. The studied area is situated between latitudes 23°10' and 23°30' N and longitudes 35°10' and 35°35' E (Figure 1).

This region is characterized by a diverse range of rock units spanning from the Precambrian to the Quaternary (Figure 2). The exposed Precambrian basement rocks in Wadi Rahba are part of the Pan-African belt within the Arabian Nubian Shield, with gneisses being the oldest rock type found in the northwestern section of the mapped area. These gneisses include three main varieties: biotite gneisses, biotite-hornblende gneisses, and hornblende gneisses, providing insights into the geological history of the region [32–33]. Ophiolites, metavolcanics, older granites, tonalites, granodiorites, monzogranites, and alkali feldspar granites are also recorded in the study area [34]. In contrast, the Quaternary deposits represent the more recent geological formations in Wadi Rahba, dating from the Pleistocene to the present (Figure 2). These deposits vary in thickness from 2 to 20 meters, generally increasing towards the Red Sea coast [35]. Composed primarily of beach sand and gravel terraces, the Quaternary deposits also include rock fragments derived from the underlying basement rocks. This mixture of sedimentary materials highlights the dynamic geological processes that play in the area and underscores the potential for valuable mineral resources, including titanite and ilmenite, within these placer deposits [36–37]. The Samples were collected from excavated pits and were taken by applying an auger sampler, each approximately 50 cm in diameter and 70 to 100 cm deep, spaced at intervals of 1 to 3.5 kilometres (Figure 1).

2.2. Spatial interpolation methods

According to Figure 1, there is a limited number of sample points covering the study area. Therefore, spatial interpolation methods are needed to create

detailed and continuous distribution maps by estimating (predicting) the missing values between the given data points. This study used Ordinary Kriging (OK) and Inverse Distance Weighting (IDW) methods to estimate mineral concentrations at unsampled locations from their neighbouring data points and create distribution maps. OK is a geostatistical interpolation technique that takes into consideration the distance and correlation between points and assumes a constant but unknown mean throughout the search area surrounding the point, while IDW is a deterministic interpolation technique that calculates the unknown values by assigning weights such that the nearby points are more heavily weighted based on their distance [38–42].

OK is suitable for complex data structures and decreases the interpolation error based on the spatial correlation between data points. Whereas IDW is relatively fast, straightforward and simple to implement. Moreover, IDW produces smooth distribution maps. On the other hand, OK requires evaluating the semi-variogram model each time and choosing the appropriate one to achieve accurate results, while IDW is oversensitive to outliers.

The accuracy of these methods was assessed by comparing measured and predicted values, using Mean Error (ME) to measure prediction bias (positive values indicate overestimated and negative values indicate underestimated) and Root Mean Square Error (RMSE) to evaluate precision and sensitivity. In addition to the output results from the semi-variogram model [40,42]. For improved performance, ME closer to 0 is desired, and a lower RMSE indicates better accuracy.

2.3. Characterization methods

Each sample from Wadi Rahba was initially mixed thoroughly and then split into representative sub-samples for characterization tests, including grain size distribution analyses and total heavy minerals (THMs) assessment. A composite technology sample (tech. sample), weighing approximately 25 kg, was created by thoroughly mixing equal portions of each individual sample to represent the area under investigation. Various characterization tests were performed on individual sampling points as well as on the technology sample, while physical upgrading processes were implemented on the technology sample only.

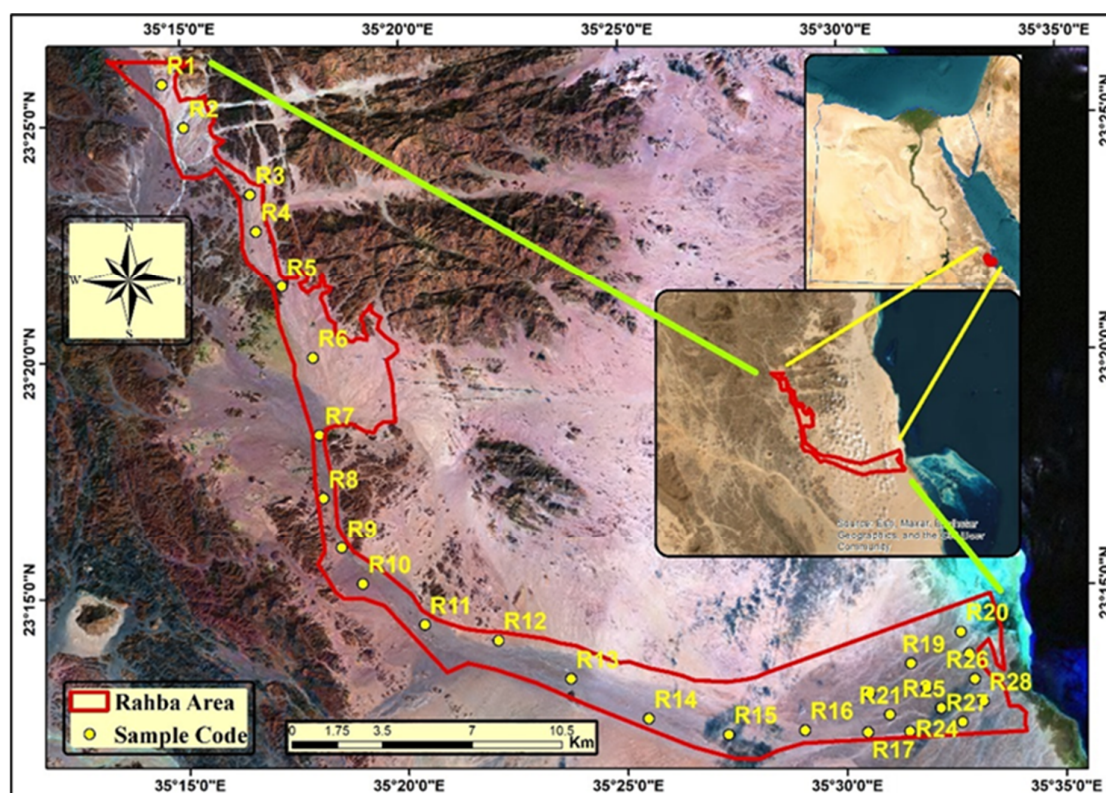


Figure 1. Satellite image showing location and sampling points of Wadi Rahba area, southeastern Desert of Egypt.

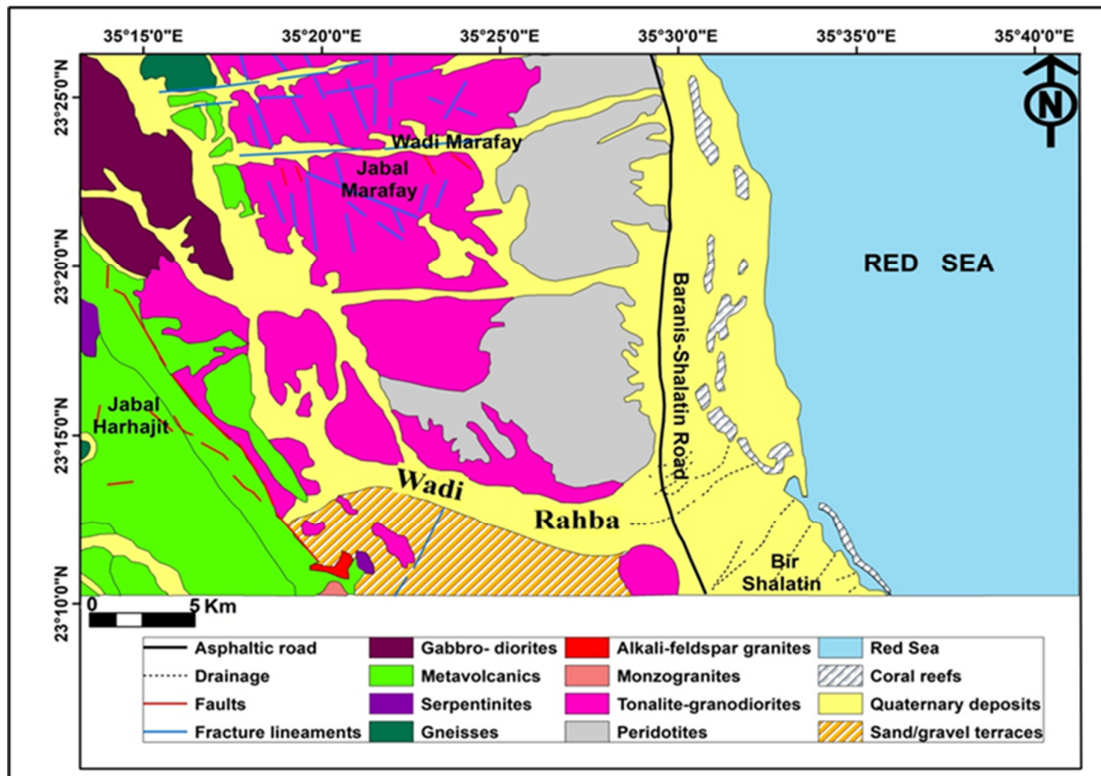


Figure 2. Geological map of the Wadi Rahba area, southeastern Desert of Egypt (Modified after [43])

2.3.1. Grain size distribution analysis

Initial analysis focused on grain size distribution, utilizing 250 g from each sampling point subjected to sieving through a series of ASTM standard sieves (2, 1, 0.5, 0.25, 0.125, and 0.063 mm) to distribute particles into gravel, very coarse sand, coarse sand, medium sand, fine sand, very fine sand, and mud sizes. To assess the THM content, heavy-liquid separation tests were conducted on a separate 100 g sample, using bromoform, which has a specific gravity of 2.89. This process allowed for the subsequent analysis of grain size distribution among the heavy minerals separated.

2.3.2. Mineralogical and chemical characterization

The mineralogical characterization of the obtained THMs was conducted using a combination of techniques, including an Olympus stereo binocular microscope, X-ray diffraction (XRD) Melvern Panalytical Empryan device model and identified phases according to PDF-2 cards release 2020, and environmental scanning electron microscopy (ESEM) equipped with energy dispersive spectrometry (EDS). Chemical assays for both the raw samples, technology sample and various magnetic fractions were performed with an energy-dispersive X-ray fluorescence (ED-XRF) Rigaku

spectrometer, employing polarized optics for enhanced accuracy.

2.4. Physical beneficiation

Wet-gravity separation was used to concentrate heavy minerals (THMs) from the Rahba placer deposits, employing Wilfley Shaking Table No. 13. The process began with an initial rougher stage, followed by two scavenging stages to recover more THMs and remove lighter silicate minerals.

- **Rougher Stage:** Operated under controlled conditions with a feed rate of 134 g/min, water flow of 14 L/min, stroke length of 1.5 cm, and an inclination of 9°.
- **Scavenging Stages:** Used more intense settings—140 g/min feed rate, 17.5 L/min water flow, 2 cm stroke length, and an 11° inclination—due to the higher proportion of light minerals at this stage.

After gravity separation, a 100 g sample from each fraction (concentrate and tailings) underwent heavy-liquid separation with bromoform to assess mineral content and material balance.

Next, the total heavy mineral concentrate (THMC) was processed using magnetic separation:

- **Low-intensity magnetic separation (LIMS)** removed magnetite.

- High-intensity magnetic separation (HIMS) via a Carpc model used to separate the remaining minerals:
 - 0.8A current separated ilmenite.
 - 3A current extracted non-magnetic titanite.

Finally, a cleaning step on the shaking table removed any remaining silicate impurities, yielding a high-purity mineral concentrate.

3. Results and Discussion

3.1. Rahba sample characterization

Grain size distribution, an essential physical parameter, was analyzed for 28 original samples and the technology sample. The results, summarized in Table 1, showed that the very coarse sand fraction was the most dominant, ranging from 10.22% to 51.62%, with an average of 32%. In the technology sample, this fraction made up 34%. The silt fraction had the lowest values, ranging from 0.04% to 5.68%, with an average of 2.26%, while the technology sample measured 2.17%.

To determine the THM content, a heavy liquid separation test was conducted using bromoform (CHBr_3 , specific gravity 2.89). After separation, the heavy and light mineral fractions were washed with acetone, dried, and weighed. The results, shown in Table 2, revealed that THM content ranged from 4.5% to 17.7%, averaging 10%, while the technology sample contained approximately 11%.

A spatial distribution map of THM content was generated using ArcGIS software (Figure 3). Interpolation methods, both geostatistical and deterministic, were applied to estimate metal concentrations at unsampled locations. This approach helps visualize mineral distribution across the region.

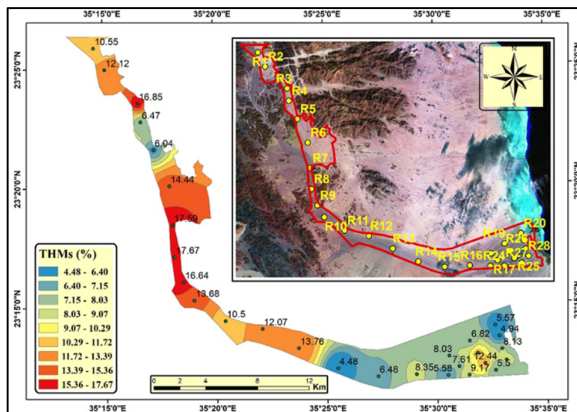


Figure 3. The spatial distribution of THMs (%) in the stream sediments samples along the Rahba area.

Detailed THM size distribution analysis was performed for each sampling point and the technology sample (Table 2). The results showed that 93% to 98.6% of THMs were concentrated in the coarse sand to very fine sand size range. The silt fraction contained 1.32% to 6.92% of THMs. Notably, the very coarse sand fraction contained no heavy minerals.

Figure 4 compares the grain size distribution of the technology sample with its THM distribution. The analysis confirmed that over 96% of THMs were found in sand fractions smaller than very coarse sand, with a significant increase in the fine and very fine sand fractions. The silt fraction contained about 3.4% of the heavy minerals. This distribution indicates high potential for efficient physical separation, as the sandy grains allow easier liberation and recovery of valuable minerals during processing.

3.1.1. Heavy Mineral Characterization

The heavy mineral grains were examined for physical characteristics, using a stereo-binocular microscope, followed by SEM-EDS for precise compositional data and XRD for crystalline structure identification. These combined techniques revealed a diverse and economically significant group of heavy minerals within Rahba low-grade sample. The identified minerals include titanite (as shown in Figures 5a and 6a), ilmenite (Figure 5b and 6b), spessartine garnet (Figure 6c), magnetite and hematite (Figure 6d), zircon (Figure 5c), epidote (Figures 5d and 6e). Each of these minerals holds potential economic value, either as industrial materials or as sources of valuable metals.

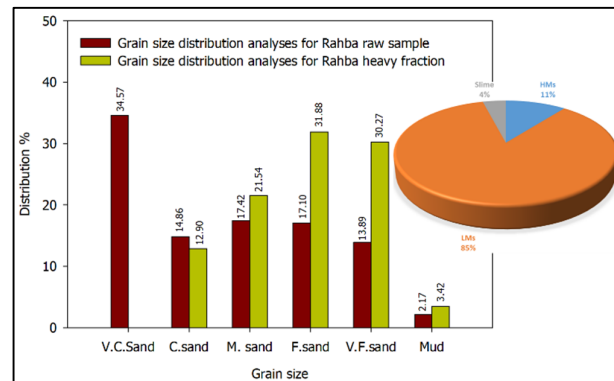


Figure 4. Grain size distribution analyses for Rahba technology sample compared to heavy mineral distribution.

Table 1. Size distribution analyses percentage for Rahba samples by weight

Sample code	Grain size distribution analyses %					
	Very coarse sand	Coarse sand	Medium sand	Fine sand	Very fine sand	Silt
R1	40.32	13.83	18.00	15.06	10.55	2.24
R2	33.52	13.63	14.36	17.75	17.27	3.47
R3	10.22	28.96	26.68	20.32	12.50	1.31
R4	51.62	16.08	12.87	9.46	8.23	1.74
R5	48.61	16.52	15.06	10.90	7.40	1.51
R6	22.68	11.59	16.69	26.84	18.91	3.29
R7	28.47	16.89	19.68	20.07	13.84	1.05
R8	19.26	8.09	24.90	28.64	17.54	1.56
R9	18.02	15.53	31.94	20.99	12.04	1.48
R10	35.11	10.15	11.44	21.93	19.42	1.96
R11	36.77	15.37	17.6	13.64	14.23	2.39
R12	41.59	14.48	14.48	15.01	12.75	1.68
R13	36.83	14.55	18.3	17.22	11.72	1.38
R14	49.46	15.06	18.04	11.18	5.86	0.41
R15	40.72	15.85	17.91	15.3	9.21	1.01
R16	32.64	13.64	18.72	18.86	13.17	2.96
R17	32.79	21.44	18.08	14.03	11.53	2.13
R18	38.14	13.33	15.55	17.26	14.97	0.75
R19	37.38	8.89	13.57	17.89	16.59	5.68
R20	35.02	11.23	15.08	16.6	17.26	4.81
R21	47.31	16.02	18.25	9.97	6.19	2.26
R22	23.23	15.99	25.71	19.61	14.07	1.39
R23	32.17	17.36	26.36	21.3	2.77	0.04
R24	22.31	12.93	17.67	23.00	19.67	4.42
R25	15.03	12.47	16.25	23.64	29.18	3.43
R26	25.18	22.13	17.91	13.85	18.37	2.56
R27	20.5	20.25	18.35	15.5	20.22	5.18
R28	21.43	21	18.67	19.31	18.28	1.31
Min.	10.22	8.09	11.44	9.46	2.77	0.04
Max.	51.62	28.96	31.94	28.64	29.18	5.68
Aver.	32.01	15.47	18.50	17.68	14.06	2.26
Tech. sample	34.57	14.86	17.42	17.10	13.89	2.17

3.1.2. Chemical assay

Spatial distribution maps showing the concentrations of major oxides such as Fe₂O₃, and TiO₂ (in percentages), along with trace elements including Cr, V, Co, Ni, and Zr (in ppm), were created using ArcGIS software and the results were displayed in Figures 7 and 8. The average composition of these elements is as follows: Fe₂O₃ ranges between 2.32% and 5.58%, with an average of 3.91%; TiO₂ varies from 0.353% to 0.72%, averaging 0.5%; and CaO ranges from 2.62% to 8.92%, with an average of 3.93%. As for the trace elements, Cr concentrations range from 90 ppm to 801 ppm, with an average of 263 ppm; V ranges from 119 ppm to 281 ppm, averaging 191 ppm; Co ranges between 93 ppm and 227 ppm, with an average of 147 ppm; Ni ranges from 64 ppm to 212 ppm, averaging 112 ppm; and Zr ranges from 131 ppm to 485 ppm, with an average of 280 ppm.

Table 3 presents the ED-XRF results for the Rahba technological sample, revealing key oxides such as 4.07% Fe₂O₃ and 0.51% TiO₂, indicating moderate iron content and low titanium presence, suggesting limited potential for titanium extraction. Among

the trace elements, zirconium (327 ppm) is the most abundant, likely due to the presence of zircon, which has industrial significance. Chromium (272 ppm), cobalt (167 ppm), and nickel (119 ppm) are also present in notable quantities, which may have applications in metallurgical processes, particularly for alloys and stainless-steel production. However, other trace elements such as zinc, yttrium, lead, copper, niobium, and tin occur in low concentrations, making them less economically viable. In summary, while the sample contains valuable trace elements like zirconium, chromium, and cobalt, the low levels of titanium and iron limit its potential for further upgrading.

The ED-XRF analysis results for major oxides and trace elements in different magnetic fractions of the representative sample from Rahba technological sample are presented in Table 3. The results show that the oversized fraction (+1mm) accounts for approximately 32.82%, while the slime after attrition is about 5.8%. The hand magnet separated fraction is around 0.16%. The magnetic fractions obtained at different current levels are as follows: 0.8A yields 2.75%, 1.5A yields 1.86%, and 2.5A yields 3.69%. The non-magnetic fraction at 2.5A

makes up about 52.87%. As shown in Table 4, the estimated content of heavy minerals, based on stoichiometric calculations, includes titanite (0.44 wt.%), ilmenite (0.15 wt.%), zircon (0.04 wt.%), spessartine garnet (0.01 wt.%), and magnetite (0.29 wt.%). In addition, the sample contains a

significant proportion of heavy silicate minerals—epidote, pyroxene, and amphiboles—totalling approximately 10.07 wt.%. These heavy minerals are accompanied by major gangue phases, primarily quartz and feldspar, which dominate the lighter mineral fraction of the sample.

Table 2. Total heavy minerals (THMs) percentage by weight in Relation to their size distribution

Sample code	THMs %	THMs size distribution in weight %					
		Very coarse sand	Coarse sand	Medium sand	Fine sand	Very fine sand	Silt
R1	10.55	0	0.96	2.77	4.09	2.40	0.34
R2	12.12	0	1.84	2.91	3.78	3.14	0.44
R3	16.85	0	3.02	5.73	5.09	2.72	0.30
R4	6.47	0	0.70	1.92	2.14	1.51	0.20
R5	6.04	0	1.24	1.74	1.93	1.04	0.09
R6	14.44	0	1.32	2.33	5.50	4.98	0.31
R7	17.59	0	3.00	4.32	5.90	4.03	0.34
R8	17.67	0	0.84	3.85	7.25	5.36	0.37
R9	16.64	0	1.47	5.03	6.21	3.59	0.34
R10	13.68	0	2.04	2.39	4.59	4.33	0.33
R11	10.5	0	1.90	2.76	3.10	2.53	0.21
R12	12.07	0	2.57	2.84	3.36	2.97	0.34
R13	13.76	0	2.14	3.25	4.86	3.33	0.18
R14	4.48	0	0.87	0.81	1.52	1.19	0.09
R15	6.48	0	0.78	0.99	2.47	2.13	0.10
R16	8.35	0	0.92	1.56	3.11	2.49	0.27
R17	5.58	0	0.72	0.75	1.74	2.22	0.14
R18	8.03	0	0.69	1.27	2.51	3.31	0.26
R19	6.82	0	0.57	0.94	1.99	3.04	0.28
R20	5.57	0	0.29	0.66	2.09	2.25	0.28
R21	7.61	0	1.42	2.72	2.34	0.97	0.15
R22	11.35	0	1.26	2.99	3.96	2.74	0.40
R23	4.94	0	0.38	0.68	1.80	1.73	0.34
R24	9.17	0	0.90	1.44	2.81	3.68	0.35
R25	12.44	0	0.87	1.23	2.69	6.94	0.71
R26	8.13	0	1.37	1.36	1.81	3.32	0.28
R27	5.5	0	0.47	0.71	1.41	2.72	0.18
R28	8.33	0	1.36	1.13	2.08	3.63	0.15
Min.	4.48	0	0.21	0.44	0.97	0.57	0.06
Max.	17.67	0	3.76	6.32	7.25	9.86	1.22
Aver.	10.04	0	1.28	2.07	3.25	3.14	0.29
Tech. sample	10.54	0	1.36	2.27	3.36	3.19	0.36

3.1.3. Spatial Distribution maps of elements

Distribution maps offer significant benefits, such as visualizing spatial patterns to facilitate the identification of trends and anomalies. They support scientific research through the analysis of spatial relationships.

The interpolation methods are carried out using the Geostatistical Analyst extension in ArcGIS Desktop 10.8 software. To assess the accuracy of these methods: sequentially remove a data point (one at a time), estimate the value of it from the remaining predicted values, and then compare the estimated value with the actual measured value. This technique is commonly used to select the most suitable semi-variogram model for OK and to determine the optimal parameters for IDW to achieve the optimal result. To compare them, ME and RMSE derived from the

differences between predicted and measured values are used as performance metrics.

For OK, certain parameters are kept constant, such as the neighbourhood type, which is set to standard, with a maximum of 5 neighbours and a minimum of 2 neighbours (number of data points) included in each sector. However, the sector type differs from one element to another. For IDW, parameters are also kept constant, with the neighbourhood type set to standard, and a maximum of 15 neighbours and a minimum of 10 neighbours (data points) in each sector. Similar to OK, the sector type changes based on the specific element. Table 5 shows the performance metrics of the elements studied for the two methods. The value of the RMSE (an indicator of the interpolation accuracy) shows that OK was better for Fe₂O₃ and TiO₂, whereas IDW was better for CaO, Cr, V, Co, Ni, Zr, and THMs, as illustrated in Figures 3, 7 and 8.

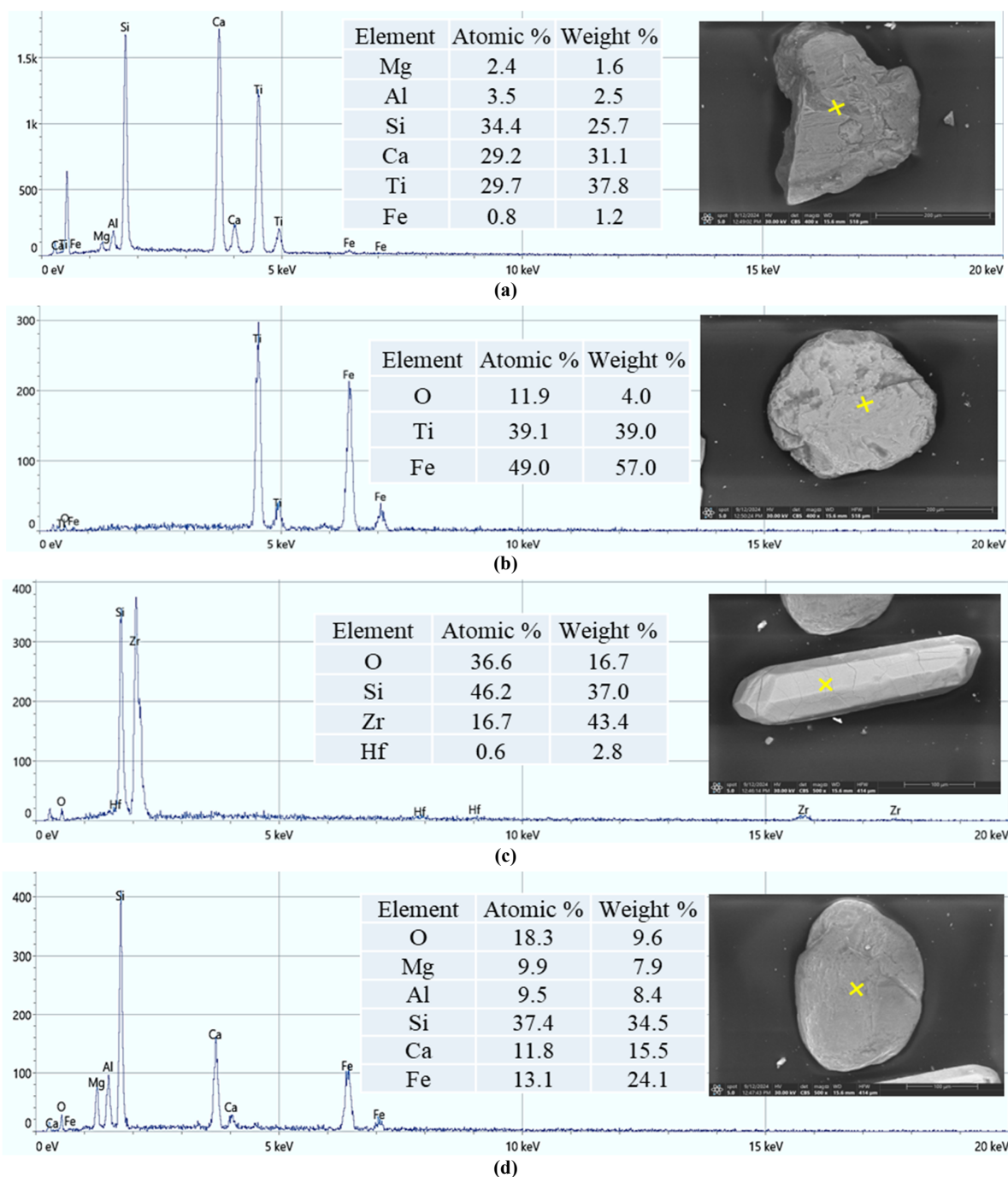


Figure 5. Back-Scattered Electron (BSE) images and corresponding EDS Spectra for Titanite (a), Ilmenite (b), Zircon (c), and Epidote (d).

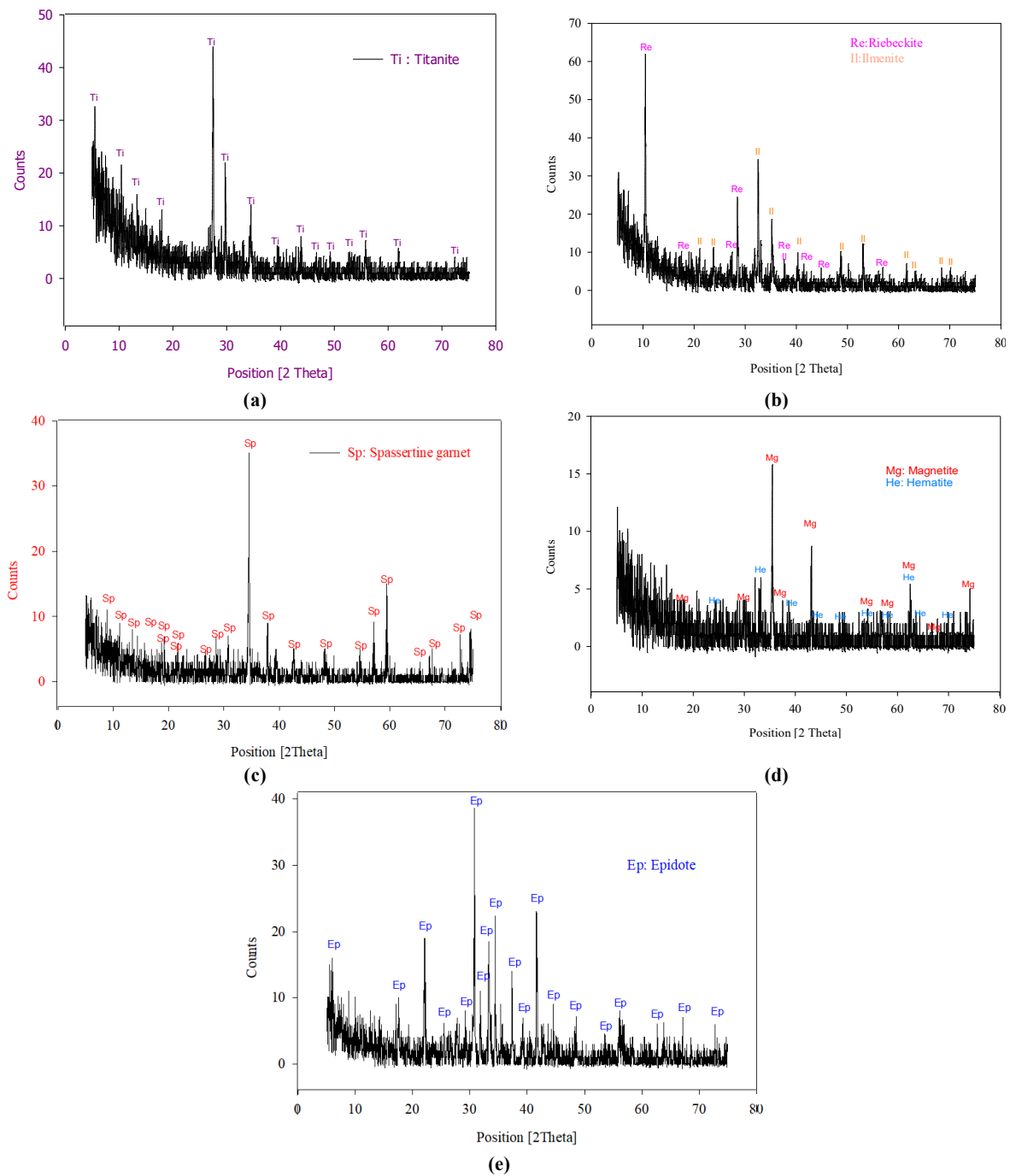


Figure 6. XRD patterns of heavy mineral content for Rahba sample, a. Titanite, b. Ilmenite and Riebeckite, c. Spessartine, d. Magnetite and Hematite, e. Epidote

Table 3. ED-XRF analyses of Rahba technology sample and their related different magnetic fractions.

Elemental analyses	Technology sample	Ilmenite-rich fraction	Garnet-rich fraction	Epidote-rich fraction	Titanite-rich fraction
Major elemental oxides in %					
Fe ₂ O ₃	4.07	14.6	10.7	10.00	1.91
CaO	4.1	2.92	4.3	4.74	3.1
TiO ₂	0.51	2.24	1.36	1.2	0.266
P ₂ O ₅	0.08	0.08	0.085	0.08	0.089
K ₂ O	1.39	0.403	0.614	0.665	1.36
MnO	0.08	0.195	0.237	0.214	0.045
Trace elements in ppm					
Cr	272	1770	547	327	86
Zr	327				
Ni	119	686	254	171	46
Co	167	532	339	257	69
V	207	532	398	261	114
Zn	70	191	176	163	51
Y	30	31	44	50	22
Pb	15.7	17	13	13	14
Cu	27	75	72	57	21

Table 4. Mineralogical composition of the Rahba technology sample

Mineral content	Wt. %	Mineral content	Wt. %
Titanite	0.44	Magnetite	0.29
Ilmenite	0.15	Heavy silicate minerals	10.07
Zircon	0.04	Gangue minerals (quartz and feldspar)	89
Garnet	0.01		

Table 5. Performance metrics

Elemental Oxides/ Elements	OK		IDW	
	ME	RMSE	ME	RMSE
Fe ₂ O ₃ %	0.008308876	0.873542869	-0.038854116	0.887515686
CaO %	-0.006641339	1.673435634	-0.035270693	1.612895746
TiO ₂ %	0.00461822	0.093324503	-0.003308667	0.098820897
Cr (ppm)	9.483952376	122.3426461	6.387024138	121.3969566
V (ppm)	-0.649695156	49.61121026	0.610039546	44.94443425
Co (ppm)	-1.370161812	39.87562974	-1.584482518	36.8672458
Ni (ppm)	-1.246985465	40.73955875	-0.828936328	37.13556109
Zr (ppm)	-2.279058036	80.28419179	-3.439334067	79.79398135

3.2. Separation Processes

3.2.1. Gravitative concentration

Upon completion of the gravity concentration processes, including both the rougher and scavenger stages, a detailed analysis was performed. The results are summarized in Table 6. The findings demonstrated that the scavenging process played a crucial role in improving recovery rates. Specifically, the recovery rate increased significantly, rising from 65.83% in the rougher

stage to 78.95% after the scavenging stages, underscoring the effectiveness of the scavenging process in maximizing heavy mineral recovery. Finally, the gravity separation process significantly enhanced the THM grade, increasing it from 10.45% in the Rahba technology sample to 33.22% in the final concentrate after the scavenging and roughing stages. This improvement was achieved with a recovery rate of 78.95% for THMs and a concentrate yield of 24.95%, demonstrating the effectiveness of the separation technique.

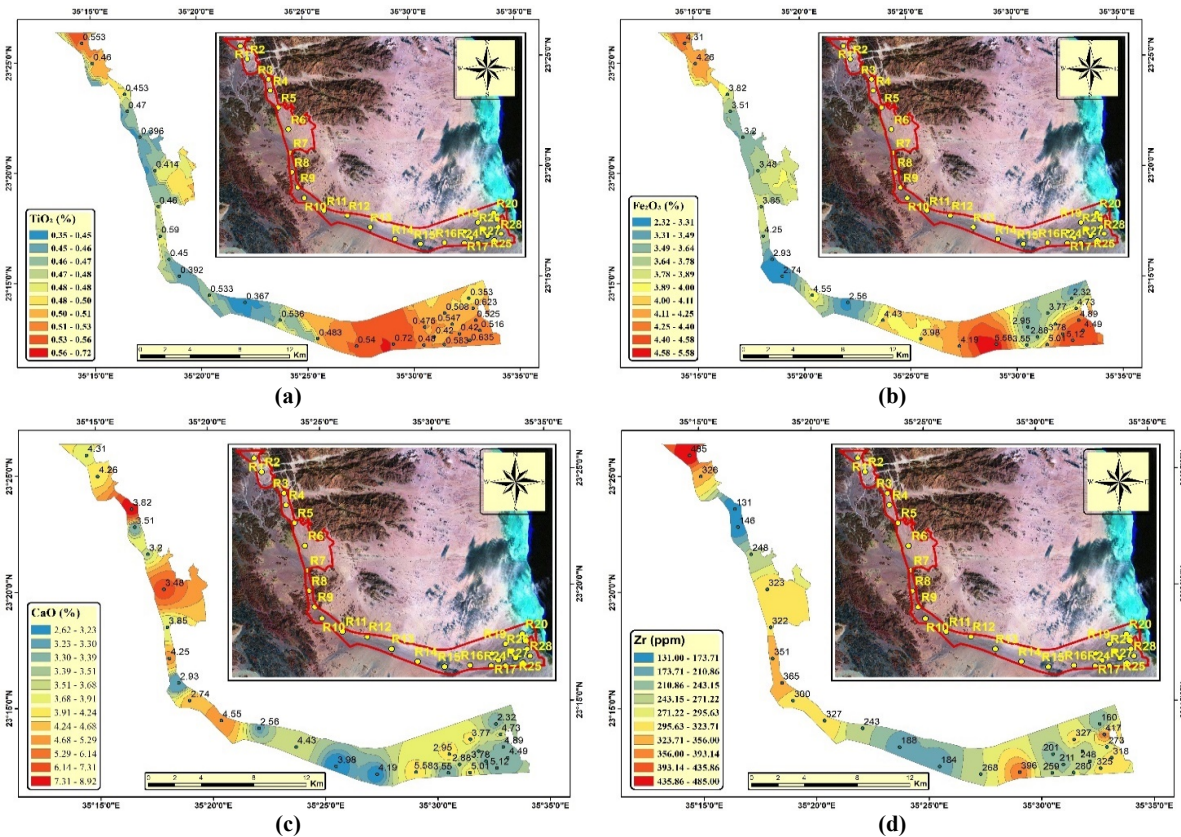


Figure 7. The spatial distribution of TiO_2 (a), Fe_2O_3 (b), CaO (c), and Zr (d) in the stream sediments samples along the Rahba area.

Table 6. Material balance of gravity concentration processes via shaking table for Rahba technology sample.

Products of tabling		Yield (%)	HMs Assay (%)	HMs Recovery (%)
Concentrate	Roughing stage	20.46	33.91	65.83
	Scavenging round 1	2.88	28.8	7.87
	Scavenging Round 2	1.61	34.38	5.25
	Total Concentrate	24.95	33.22	78.95
Tail	Total	75.05	2.99	21.05
Feed	Total	100	10.54	100

3.2.2. Magnetic Separation

This step aims to produce high purity concentrates of ilmenite and titanite from the THM concentrate obtained via the shaking table, resulting in separate ilmenite and titanite concentrate fractions.

Ilmenite-concentrate Fraction (ICF)

At this fraction, the focus was on ilmenite as the main mineral of interest. Using HIMS at 0.8A current intensity, 1.4% of the THMC was separated as a magnetic fraction. SEM-EDS analysis (shown in Figure 9a) revealed that the dominant elements were iron, titanium, and silicon, confirming ilmenite as the primary mineral, along with some traces of spessartine garnet. An analysis of separate ilmenite grains is shown in Figure 9b and c. ED-XRF analysis results, presented in Table 7,

confirmed that gravity and magnetic separation effectively increased ilmenite assay from 0.11% in the raw sand to 6.16% in the concentrate, with a recovery rate of 79% and a mass yield of 1.41%.

Titanite-concentrate fraction (TCF)

This refers to the non-magnetic fraction at 3A current intensity that comprises 17.17% mass of the THMC. The BSE-EDS data (Figure 10a) revealed key elemental contents, including silicon, titanium, zirconium, and calcium, SEM-EDS data in Figure 10b confirmed titanite is the dominant mineral in this fraction with traces of zircon (Figure 10c). The results from ED-XRF analysis (Table 7) showed that the titanite content increased significantly during processing. In the raw sand, titanite made up 0.44%, but after separation, the titanite content rose

to 2.18% in the concentrate. The recovery rate of titanite from the original material was 85.08%, with a mass yield of 17.17%, demonstrating the effectiveness of the separation process in concentrating titanite from the Rahba placer deposit.

The Titanite-Concentrate Fraction (TCF) underwent further purification steps using a shaking table to remove silicate minerals, which were present as impurities. This process successfully produced a more refined titanite concentrate, resulting in a yield of up to 1.58%.

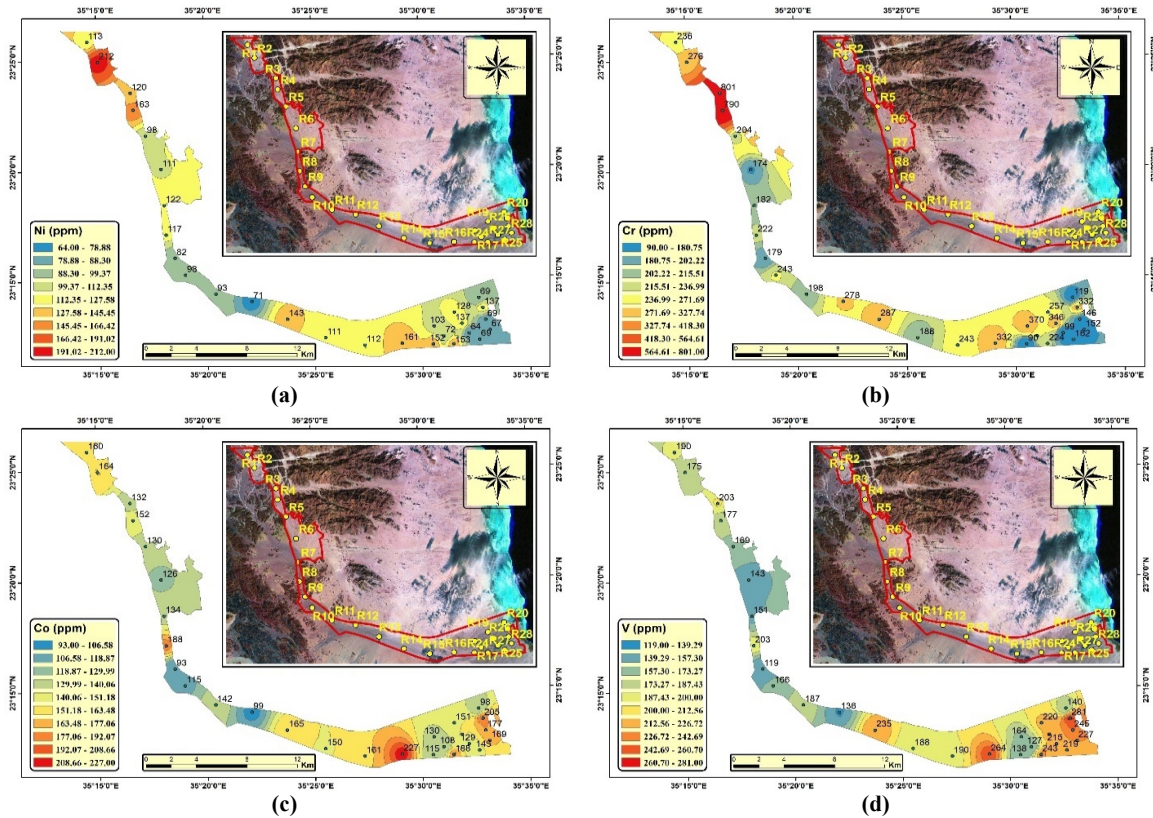


Figure 8. The spatial distribution of Ni (a), Cr (b), Co (c), and V (d) in the stream sediments samples along the Rahba area.

Table 7. ED-XRF analyses results of both ilmenite (ICF) and titanite (TCF) concentrate fractions of Rahba placer deposits

Elemental analyses	ICF	TCF
Major oxides in %		
Fe ₂ O ₃	13.9	1.85
CaO	3.66	3.67
TiO ₂	3.24	0.66
P ₂ O ₅	0.09	0.10
K ₂ O	0.31	1.3
MnO	0.28	0.04
Trace elements in ppm		
Cr	2080	76
Zr	109	504
Ni	539	49
Co	508	77
V	832	130
Zn	169	46
Y	44	37
Pb	11	14.4
Cu	95	17
Nb	6	24

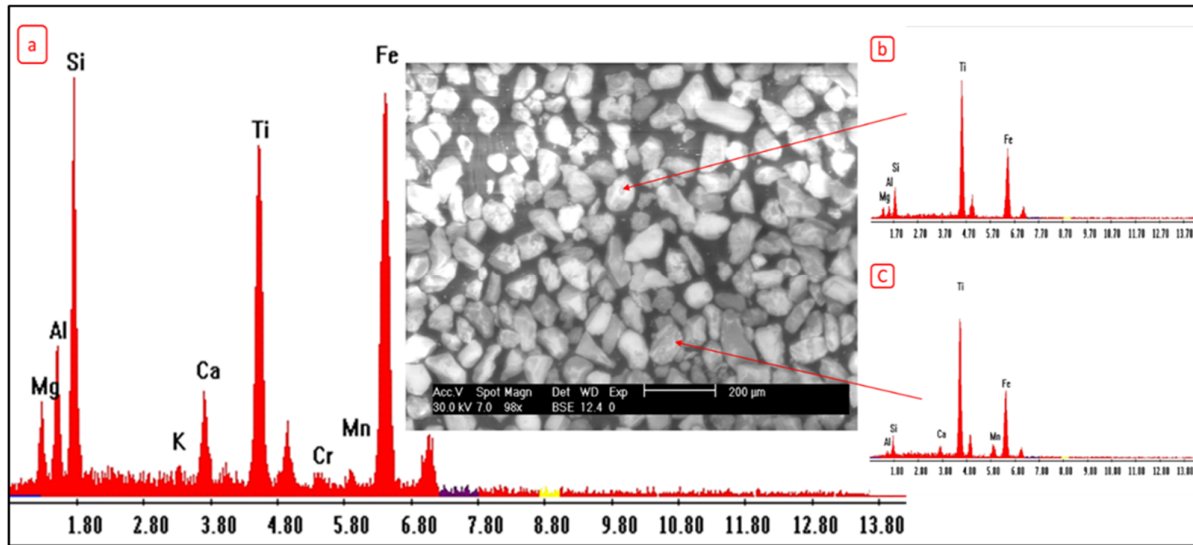


Figure 9. BSE image and corresponding EDS spectra for; ilmenite-rich fraction (a), ilmenite (b), (c)

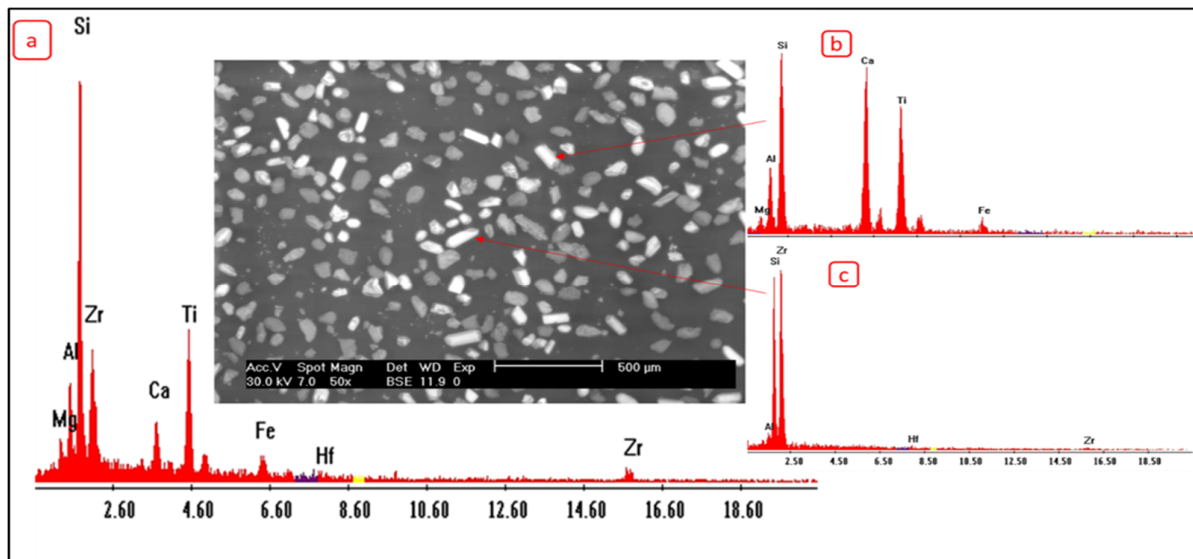


Figure 10. BSE image and corresponding EDS spectra for; titanite-rich fraction (a), apatite (b), zircon (c)

4. Conclusions

This study presents a comprehensive assessment of the heavy mineral potential of low-grade placer deposits in Wadi Rahba, located along Egypt's southern Red Sea coast. Emphasis was placed on the recovery of economically significant minerals—particularly ilmenite and titanite—which are critical for titanium production and other industrial applications. The region is underlain by a complex geological framework comprising Precambrian basement rocks and Quaternary sediments, favouring heavy mineral enrichment.

A systematic sampling program was conducted, and mineralogical characterization of both individual and composite samples was performed using grain size analysis, heavy mineral separation, XRD, SEM-EDS, and ED-XRF. The results revealed a varied assemblage of heavy minerals including titanite, ilmenite, zircon, magnetite, spessartine garnet, and epidote, as well as high levels of heavy silicate gangue minerals.

A two-stage beneficiation process—comprising wet gravity separation followed by magnetic separation—proved highly effectively. Gravity separation yielded a concentrate containing 33.22% total heavy minerals, with a recovery rate of 78.95%. Subsequent magnetic separation significantly enriched the target minerals: ilmenite content rose from 0.11% to 6.16% (79% recovery), and titanite increased from 0.44% to 2.18% (85.08% recovery).

The successful implementation of these physical upgrading techniques highlights their value in mineral processing, especially for low-grade placer resources. Their eco-friendly and energy-efficient nature, compared to chemical processing methods, enhances the sustainability of the extraction process and supports responsible mineral resource management. This position is the Wadi Rahba deposits as a viable and environmentally conscious resource for future exploitation.

Further investigations are recommended to characterize the concentrate fractions in greater detail, evaluate the

economic viability of full-scale production, and assess the environmental and social implications of industrial development in the area. Overall, this study provides critical insights into the beneficiation potential of Wadi Rahba sediments and lays a scientific foundation for their sustainable utilization as a source of critical minerals.

References

- [1]. Shengo, M., Ilunga, F., & Mambwe Matanda, P. (2024). Linking ores flotation results to the Kinsenda copper deposit mineralogical features: enhancing the recovery of copper retained in flotation tailings. *Canadian Metallurgical Quarterly*, 1–15. 64(3), 1374–1388.
- [2]. Wani, O. B., Khan, S., Shoaib, M., da Costa Gonçalves, C., Chen, Z. Zeng, H., & Bobicki, E. R. (2024). Processing of low-grade ultramafic nickel ores: A critical review. *Minerals Engineering*, 218, 108976.
- [3]. Bulayani, M., Raghupatruni, P., Mamvura, T., & Danha, G. (2024). Exploring Low-Grade Iron Ore Beneficiation Techniques: A Comprehensive Review. *Minerals*, 14(8), 796.
- [4]. Bruckard, W.J., Pownceby, M.I., Smith, L.K., & Sparrow, G.J. (2015). Review of processing conditions for Murray Basin ilmenite concentrates. *Mineral Processing and Extractive Metallurgy*, 124 (1), 47-63.
- [5]. Mudd, G.M., & Jowitt, S.M. (2016). Rare earth elements from heavy mineral sands: assessing the potential of a forgotten resource. *Applied Earth Science*, 125 (3), 107-113.
- [6]. Klein, C., & Philpotts, A. (2013). Earth Materials: Introduction to Mineralogy and Petrology. *Cambridge University Press*, 536.
- [7]. Khedr, M.Z., Zaghloul, H., Takazawa, E., El-Nahas, H., Azer, M.K., & El-Shafei, S.A. (2023). Genesis and evaluation of heavy minerals in black sands: A case study from the southern Eastern Desert of Egypt. *Geochemistry*, 83 (1), 125945.
- [8]. Abdel-Karim, A., Zaid, S.M., Moustafa, M.I., & Barakat, M.G. (2016). Mineralogy, chemistry and radioactivity of the heavy minerals in the black sands, along the northern coast of Egypt. *Journal of African Earth Sciences*, 123, 10–20.
- [9]. Samy, Y., & El-Gohary, A. (2013). Heavy Minerals Pattern and Indices as a Guide for Provenance and Transportation of Beach Sands along the Northern Sinai Coast, Egypt. *Journal of Applied Sciences Research*, 9 (11), 5656-5664.
- [10]. El-Kammar, A.A., Ragab, A.A., & Moustafa, M.I. (2011). Geochemistry of Economic Heavy Minerals from Rosetta Black Sand of Egypt. *JAKU: Earth Science*, 22(2), 69–97.
- [11]. Fawzy, M.M., Abu El Ghar, M.S., Gaafar, I.M., El Shafey, A.M., Diab, M., & Hussein, A.W. (2022a). Diit Quaternary Stream Sediments, Southern Coast of the Red Sea, Egypt: Potential Source of Ilmenite, Magnetite, Zircon, and Other Economic Heavy Minerals. *Mining, Metallurgy & Exploration*, 39 (2), 655–667.
- [12]. Fawzy, M.M., Abu El Ghar, M.S., Gaafar, I.M., El Shafey, A.M., Diab, M., & Hussein, A.W. (2022b). Recovery of valuable heavy minerals via gravity and magnetic separation operations from Diit Quaternary stream sediments, southern coast of the Red Sea, Egypt. *Journal of Physics: Conference Series*, 2305(1), 1-14.
- [13]. Fawzy, M., Bayoumi, M., Shahin, H., Emad, B., El Shafey, A.H., Abdel-Azeem, M., Ismail, A., El-Moghazy, A., & Diab, M. (2024a). Economic heavy minerals in the stream sediments of wadi Shaab, southern coast of the Red Sea, Egypt; characterization and upgrading for investigation of their potential recovery. *Bulletin of the Mineral Research and Exploration*, 174 (174), 145-165.
- [14]. Fawzy, M., Bayoumi, M., Shahin, H., Emad, B., El Shafey, A.H., Abdel-Azeem, M., Ismail, A., & Diab, M. (2024b). Characterization and beneficiation potential for valuable heavy minerals from Wadi Ibib stream sediments, southern coast of the Red Sea, Egypt. *International Journal of Mining and Geo-Engineering*, 58 (4), 371-381.
- [15]. Titanium Mill Products - Global Strategic Business Report, (2025). *Global Industry Analysts, Inc*, 197 Pages. ID: 5141513. <http://www.researchandmarkets.com/reports/5141513>.
- [16]. Laxmi, T., Srikant, S.S., Rao, D.S., & Bhima Rao, R. (2013). Beneficiation studies on recovery and in-depth characterization of ilmenite from red sediments of badlands topography of Ganjam District, Odisha, India. *International Journal of Mining Science and Technology*, 23(5), 725–731.
- [17]. Fawzy, M., Mahdy, N., & Mabrouk, S. (2020). Mineralogical characterization and physical upgrading of radioactive and rare metal minerals from Wadi Al-Baroud granitic pegmatite at the Central Eastern Desert of Egypt. *Arabian Journal of Geosciences*, 13, 413.
- [18]. Fawzy, M.M., Kamar, M.S., & Saleh, G.M. (2021). Physical processing for polymetallic mineralization of Abu Rusheid mylonitic rocks, South Eastern Desert of Egypt. *International Review of Applied Sciences and Engineering*, 12 (2), 134–146.
- [19]. Zhang, S., Rao, M., Xiao, R., You, J., Li, G., & Jiang, T. (2022). Enrichment of Nb and Ti from carbonatite pyrochlore ore via calcining-slaking followed by gravity separation. *International Journal of Mining Science and Technology*, 32(3), 615–626.
- [20]. Zhu, F., Ma, Z., Qiu, K., & Peng, W. (2023). Separation of Ilmenite from Vanadium Titanomagnetite by Combining Magnetic Separation and Flotation Processes. *Separations*, 10 (2), 95.
- [21]. Kim, K., & Jeong, S. (2019). Separation of Monazite from Placer Deposit by Magnetic Separation. *Minerals*, 9 (3), 149.
- [22]. Diab, M., El Ghar, M.A., Gaafar, I.M., El Shafey, A.H.M., Hussein, A.W., & Fawzy, M.M. (2022). Potentiality of Physical Upgrading for Valuable Heavy Minerals from Sermatai Area, Egypt. *Journal of Mining and Environment*, 13 (1), 15–32.
- [23]. Nzeh, N.S., & Popoola, P.A. (2024). Physical beneficiation of heavy minerals – Part 2: A state-of-the-art

literature review on magnetic and electrostatic concentration techniques. *Heliyon*, 10 (11), e32201.

[24]. Gao, Z., Gao, Y., Zhu, Y., Hu, Y., & Sun, W. (2016). Selective Flotation of Calcite from Fluorite: A Novel Reagent Schedule. *Minerals*, 6 (4), 114.

[25]. Fawzy, M.M. (2018). Surface characterization and froth flotation of fergusonite from Abu Dob pegmatite using a combination of anionic and nonionic collectors. *Physicochemical Problems of Mineral Processing*, 54 (3), 677–687.

[26]. Fawzy, M.M. (2021). Flotation separation of dravite from phlogopite using a combination of anionic/nonionic surfactants. *Physicochemical Problems of Mineral Processing*, 57(4), 87–95.

[27]. He, J., Tang, H., Guo, C., Zhu, L., Huang, S., & Yang, B. (2024). Synergist enhancement of effective desilication of graphite ore by rotary triboelectric separation and surface modification. *Powder Technology*, 444, 119965.

[28]. Yang, B., & He, J. (2025). New insights into selective depression mechanism of Tamarindus indica kernel gum in flotation separation of fluorapatite and calcite. *Separation and Purification Technology*, 354, 128787.

[29]. Rubio, J., Souza, M.L., & Smith, R.W. (2002). Overview of flotation as a wastewater treatment technique. *Minerals Engineering*, 15(3), 139–155.

[30]. Thejas, H.K., & Hossiney, N. (2022). A short review on environmental impacts and application of iron ore tailings in development of sustainable eco-friendly bricks. *Materials Today: Proceedings*, 61, 327–331.

[31]. De Haes, S., Lucas, P., & Haes, S. de. (2024). Environmental impacts of extraction and processing of raw materials for the energy transition. *The Hague: PBL Netherlands Environmental Assessment Agency*, 40.

[32]. Sabet, A.H. (1972): On the stratigraphy of the basement rocks of Egypt. *Ann. Geol. Surv. Egypt*, V. II.

[33]. Saleh, G.M., Dawoud, M.I., Shahin, H.A., Khaleal, F.M., & Emad, B.M. (2018). Gabal El Fereyid - Wadi Rahaba area, South Eastern Desert, Egypt: mineralization and spectrometric prospecting. *International Journal of Mining Science (IJMS)*, 4 (2), 1-15.

[34]. El Baraga, M.H. (1992). Geological, mineralogical and geochemical studies of the Precambrian rocks around Wadi

Rahaba, South Eastern Desert, Egypt. *PhD Geol, Faculty of Science, Tanta University, Egypt*, 278.

[35]. Abdel Moneim, A.A. (2005). Overview of the geomorphological and hydrogeological characteristics of the Eastern Desert of Egypt. *Hydrogeology Journal*, 13, 416-425.

[36]. Yousef, A.F., Salem, A.A., Baraka, A.M., & Aglan, O.Sh. (2009). The impact of geological setting on the groundwater occurrences in some wadis in Shalatein-Abu Ramad area, South Eastern Desert, Egypt. *European Water*, 25 (26), 53-68.

[37]. Shawky, H.A., Said, M.M., El-Aassar, A.M., Kotp, Y.H., & Abdel Mottaleb, M.S.A. (2012). Study the chemical characteristics of groundwater to determine the suitable localities desalination processes in the area between Mersa Alam and Ras Banas, Red Sea Coast Eastern Desert, Egypt. *Journal of American Science*, 8(11), 93-106.

[38]. Maliva, R.G. (2016). Geostatistical Methods and Applications. In: *Aquifer Characterization Techniques. Springer Hydrogeology*, 595-617.

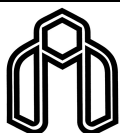
[39]. Karwariya, S., Dey, P., Bhogal, N.S., Kanga, S., & Singh, S.K. (2021). A Comparative Study of Interpolation Methods for Mapping Soil Properties: A Case Study of Eastern Part of Madhya Pradesh, India. In: *Rai, P.K., Singh, P., Mishra, V.N. (eds) Recent Technologies for Disaster Management and Risk Reduction*, 431-449.

[40]. Liu, Z., & Yan, T. (2021). Comparison of Spatial Interpolation Methods Based on ArcGIS. *Journal of Physics: Conference Series*, 1961 012050.

[41]. Usowicz, B., Lipiec, J., Łukowski, M., & Słomiński, J. (2021). Improvement of Spatial Interpolation of Precipitation Distribution Using Cokriging Incorporating Rain-Gauge and Satellite (SMOS) Soil Moisture Data. *Remote Sensing*, 13 (5), 1039.

[42]. Boumpoulis, V., Michalopoulou, M., & Depountis, N. (2023). Comparison between Different Spatial Interpolation Methods for the Development of Sediment Distribution Maps in Coastal Areas. *Earth Science Informatics*, 16, 2069–2087.

[43]. EGSMA (1999). Egyptian geological survey and mining; Geologic Map of Baranis, Quadrangle, Egypt, scale 1:250 0000. *Geol. Surv. Cairo, Egypt*.



دانشگاه صنعتی شاهرود

نشریه مهندسی معدن و محیط زیست

نشانی نشریه: www.jme.shahroodut.ac.ir

انجمن مهندسی معدن ایران

بازیابی بهینه و پایدار ایلمنیت و تیتانیت از ذخایر کم عیار پلاسور رحبا: ادغام تکنیک‌های غنی‌سازی فیزیکی

مونا فوزی^{۱*}، مهیناز شوقی^۲، احمد اسماعیل^۳، مصطفی بیومی^۴، حسن شاهین^۵، بها عماد^۶، احمد عربی^۷، جهان علی^۸، احمد عبدالموتی^۹ و محمد دیاب^{۱۰}

۱. اداره ارتقاء فیزیکی، بخش تولید، اداره مواد هسته‌ای. صندوق پستی ۵۳۰، معادی، قاهره، مصر
۲. اداره قراردادهای، بخش قراردادهای و توافق‌نامه‌ها، اداره مواد هسته‌ای. صندوق پستی ۵۳۰، معادی، قاهره، مصر
۳. اداره کانی‌شناسی، بخش تحقیقات، اداره مواد هسته‌ای. صندوق پستی ۵۳۰، معادی، قاهره، مصر
۴. اداره سنجش از دور، بخش قراردادهای و توافق‌نامه‌ها، اداره مواد هسته‌ای. صندوق پستی ۵۳۰، معادی، قاهره، مصر
۵. اداره مطالعات، بخش قراردادهای و توافق‌نامه‌ها، اداره مواد هسته‌ای. صندوق پستی ۵۳۰، معادی، قاهره، مصر
۶. اداره سنگ‌های گرانیته رادیواکتیو، بخش تحقیقات، اداره مواد هسته‌ای. صندوق پستی ۵۳۰، معادی، قاهره، مصر
۷. اداره تجزیه و تحلیل، بخش تولید، اداره مواد هسته‌ای. صندوق پستی ۵۳۰، معادی، قاهره، مصر
۸. بخش تحقیقات، سازمان مواد هسته‌ای. صندوق پستی ۵۳۰، معادی، قاهره، مصر
۹. دانشکده کامپیوتر و اطلاعات، دانشگاه زقازیق، زقازیق، مصر
۱۰. بخش ارتقاء فیزیکی، بخش تولید، سازمان مواد هسته‌ای. صندوق پستی ۵۳۰، معادی، قاهره، مصر

چکیده

در پاسخ به افزایش تقاضای جهانی برای مواد معدنی حیاتی و نیاز به بهره‌برداری مسئولانه از منابع زیست‌محیطی، این مطالعه روش‌های بازیابی پایدار از ذخایر پلاسوری کم‌عیار در منطقه وادی رحبه در امتداد ساحل جنوبی دریای سرخ مصر را بررسی می‌کند. تمرکز بر غنی‌سازی ایلمنیت و تیتانیت به عنوان مواد معدنی ارزشمند اولیه است. بیست و هشت نمونه، از جمله یک نمونه فناوری کامپوزیت، با استفاده از تکنیک‌های XRD، SEM-EDX و ED-XRF مورد تجزیه و تحلیل قرار گرفتند. نتایج نشان می‌دهد که محتوای کل کانی‌های سنگین (THM) از ۴.۵٪ تا ۱۷.۷٪ متغیر است که به طور متوسط تقریباً ۱۰٪ است و ۱۱٪ در نمونه کامپوزیت است. مواد معدنی ارزشمند شناسایی شده شامل تیتانیت، ایلمنیت، لوکوکسن، زیرکون، مگنتیت و روتیل، در کنار غلظت‌های بالای کانی‌های سیلیکات سنگین مانند اپیدوت، پیروکسن و آمفیبول‌ها هستند. محتوای تخمینی شامل ۰.۴۴ درصد وزنی تیتانیت، ۰.۱۵ درصد وزنی ایلمنیت و مقادیر ناچیزی زیرکون (۰.۰۴ درصد وزنی)، اسپسارتین (۰.۰۱ درصد وزنی) و مگنتیت (۰.۲۹ درصد وزنی) است. برای افزایش بازیابی، ترکیبی از تکنیک‌های جداسازی ثقلی (میز لرزان ویلفلی) و جداسازی مغناطیسی (LIMS و HIMS) به کار گرفته شد. این روش‌ها به طور مؤثر تیتانیت و ایلمنیت را تغلیظ کردند و به ترتیب به نرخ بازیابی ۸۵.۰۸ درصد و ۷۹ درصد دست یافتند. یافته‌ها، پتانسیل استخراج اقتصادی از منابع کم‌عیار را با استفاده از تکنیک‌های ارتقاء فیزیکی پایدار برای محیط زیست برجسته می‌کنند.

اطلاعات مقاله

تاریخ ارسال: ۲۰۲۵/۰۵/۱۲

تاریخ داوری: ۲۰۲۵/۰۶/۰۵

تاریخ پذیرش: ۲۰۲۵/۰۸/۰۶

DOI: 10.22044/jme.2025.16225.3141

کلمات کلیدی

ایلمنیت
تیتانیت
غلظت گرانی
جداسازی مغناطیسی
رحبا